Eng. Sci., 2022, **20**, 199–208

Engineered Science

DOI: https://dx.doi.org/10.30919/es8e698

Design of Self-Wetting Interface between Garnet Solid Electrolyte and Lithium Metal Electrode

Haiquan Zhang,[1,#] Houji Liu,[1,#] Junping Mai,[1,#] Yuxi Ren,[1] Renjuan Wang,[1] Xin Li,[1] Qijiu Deng[1,2], Rui-Zhi Zhang[3] and Ning Wang[1,*]

Abstract

Solid-state lithium metal batteries have emerged as promising energy storage systems due to large energy storage density and low-risk safety hazard. However, high-interface resistance between the garnet-based electrolyte and Li metal anode is one of the major challenges for all-solid-state batteries. Herein, a straightforward modification method is reported, rather than relying on hot pressing under an inert atmosphere or high-cost fabrication techniques to produce metastable nano-coating on garnet electrolyte surface. Fresh Li metal/cobalt-modified solid-state electrolyte/Li metal batteries are placed at room temperature for 48 hours under a tiny pressure of 1 MPa, however the interfacial resistance between the garnet and Li metal reduces from 5,800 – 8,200 Ω cm^2 to only 162 Ω cm^2. At a current density up to 1.6 mA cm^{-2}, the symmetrical batteries exhibit a stable signal voltage of about 190 mV. The maximum voltage fluctuation is less than 7 mV for the batteries during 160 Li-striping/plating cycles at 0.25 mA cm^{-2}. Excellent electrochemical performance and easy-to-industrial modification method are beneficial for the commercialization of Li metal all-solid-state batteries.

Keywords: Li metal battery; Garnet solid-state electrolyte; Interfacial resistance; Li-ion conductivity.
Received: 24 March 2022; Revised:18 April 2022; Accepted: 18 April 2022.
Article type: Research article.

1. Introduction

Lithium metal anode is obvious attractive in enhancing the storage energy density of rechargeable batteries due to the highest theoretical specific capacity (3860 mAh g^{-1}) and lowest redox potential (−3.05 V versus standard hydrogen electrode). The main obstacle to large-scale application is the high-risk safety hazards of the Li metal anode, based on the inevitable formation of Li dendrites on the anode during the electrodeposition process.[1-5] The Li metal dendrites undergo irreversible exothermic reactions with liquid electrolytes, resulting in low Coulombic efficiency and short cycle life of Li-ion batteries. On the other hand, Li dendrites penetrate into the electronically insulated separator and cause internal short circuits. A large number of strategies have been developed to address the challenge of the Li metal dendrites, such as the use of 3D architectural structured current collectors to reduce the uneven deposition of Li metal caused by tip discharge,[6,7] mixing electrolytes with additives to form a protective layer,[8,9] increasing the salt content of the electrolyte,[10] and using non-combustible ionic liquids[11,12] to replace conventional carbonate solvents. Inhibiting the formation of Li metal dendrites at high current densities remains a continuing challenge for liquid Li metal batteries.

Compared with liquid electrolyte batteries, solid-state batteries have considerable advantages in suppressing Li dendrite formation/penetration and improving thermal/chemical stability. A large number of solid-state electrolytes (SSEs) have been investigated, such as sulfide Li_3PS_4,[13,14] hydride $LiAlH_4$,[15] halide Li_2CdI_4,[16] perovskite $Li_{0.34}La_{0.51}TiO_{2.94}$,[17] phosphate $LiGe_2(PO_4)_3$[18,19] and $Li_{1.3}Al_{0.3}Ti_{1.7}(PO_4)_3$,[20] and LiPON.[21,22] A good alternative to these SSEs is the garnet-type oxides with general formula $A_3B_2C_3O_{12}$ where *A*-, *B*-, *C*- sites have dodecahedral (D_d), octahedral (O_h), and tetrahedral (T_d) coordinations, respectively. Garnet $Li_7La_3Zr_2O_{12}$ (LLZO)[23-27] electrolyte is very attractive for solid-state Li-ion batteries, as it features the advantages of low sintering temperature, stability toward Li metal, wide voltage window (0–6 V), and high ionic

[1] *State Key Laboratory of Marine Resource Utilization in South China Sea, Hainan University Haikou, 570228, China.*
[2] *International Research Center for Composite and Intelligent Manufacturing Technology, School of Materials Science and Engineering, Xi'an University of Technology, Xi'an, 710048, China.*
[3] *School of Engineering and Materials Science, Queen Mary University of London, London E1 4NS, UK.*
[#] *These authors contributed to this work equally.*
**E-mail:* wangn02@foxmail.com (N. Wang)

conductivity at room temperature (10^{-3} – 10^{-4} S cm^{-1}). One of major challenges is the large interfacial resistance between garnet electrolyte and Li metal electrode due to the poor wettability of the garnet electrolyte against molten Li electrode. Hot-pressed Li metal has a very limited reduction in interface resistance, because it is impossible to fundamentally solve the huge energy level difference between garnet and Li metal.[28] Currently, the reported surface treatment methods of the garnet electrolyte with thin metal (*e.g.*, Al,[29] Ge[30]) or oxide coatings (*e.g.*, Al_2O_3,[31] ZnO[32])alloying (*e.g.*, Li-Si[33], Li-Mg,[34] Li-graphite[35]) surface leaning, and surface chemical treating,[36] can greatly improve the wettability of Li on the garnet SSE. However, such surface modifications based on cutting-edge manufacturing technology are only effective at the Li-buffer layer interface. It should not be ignored that the composition, structure, and ionic conductivity of the buffer layer are difficult to maintain stability under high current density or long-term electrodeposition. Stripping/plating Li metal slowly erodes the metastable buffer layer, resulting in the failure of the surface treatments.

Herein, a self-wetting interface of garnet electrolyte and Li metal electrode is designed, and leads to a significant decrease in interfacial impedance from 5,800 – 8,200 Ω cm^2 to only 162 Ω cm^2. Importantly, the high-quality contact interface is obtained through a thermodynamic spontaneous process at room temperature, resulting in a Li metal-based battery with excellent cycling and stability. The unique design is very beneficial to development of all-solid-state batteries.

2. Experimental section

2.1 Material preparation

The LLAZO powder[31-35] was synthesized via the solid-state phase sintering technique. The starting materials were Li_2CO_3 (99%, Aladdin), $La(NO_3)_3$ (99.9%, Aladdin), $ZrO(NO_3)_2$ (99.9%, Aladdin), and Al_2O_3 (99.99%, Aladdin).

Stoichiometric amounts of these chemicals were dispersed in deionized water and a 10% excess of Li_2CO_3 was added to compensate for Li volatilization during the high-temperature pellet preparation. The ball-milled mixture was evaporated at 393K for 12 hours and then calcined to 1173 K for 12 hours to synthesize the precursor powder. The powders were then pressed into pellets, which were sintered at 1323 – 1423 K for 24 hours. The sintered LLAZO pellets were polished to ~500 μm thickness with two smooth surfaces, remarked as SSE.

The fresh garnet ceramics were buried in commercial lithium cobalt oxide ($LiCoO_2$) electrode material and calcined at 873 K for 6 hours to ensure that the garnet surface was completely and uniformly doped. The modified sample was named Co@SSE@Co.

2.2 Material characterization

The surface morphology investigation was carried out on a field emission scanning electron microscope (FE-SEM, Hitachi S4800) and energy-dispersive spectroscopy mapping (EDS, Bruker Nano XFlash Detector 5030). Before the FE-SEM investigation, the samples were sputtered with gold. A Kratos AXIS-SUPRA spectrometer was used to analyze the X-ray photoelectron spectroscopy (XPS, Zetasizer Nano S90) of the materials. Powder X-ray diffraction (XRD) measurements were performed using Cu Kα (λ= 0.154056 nm) radiation with a scan rate of 4° min^{-1} and a step size of 0.03° in the 2θ range of 15° to 60°.

To measure the ionic conductivity of the garnet SSE, both sides of the ceramic pellet were coated with an Au layer, which served as a blocking electrode. Electrochemical impedance spectroscopy (EIS) was performed across a frequency range of 1 MHz to 100 mHz with a 50 mV perturbation amplitude. Conductivities were calculated using $\sigma = h/(Z \times A)$, where Z is the impedance for the real axis in the Nyquist plot, h is the garnet ceramic disc length, and A is the surface area.A thin Li foil disc (0.5 cm in diameter and 0.2 mm thick) was put on Co@SSE electrolyte pellets in a glovebox filled with ultrahigh-purity Ar (99.999%), and then the laminated devices were allowed to stand at room temperature for 48 hours under. A low pressure of 1 MPa was used to help the initial contact of Li metal electrode on the surface of garnet electrolyte. The Li metal batteries were packaged in 2032-coin cell. Electrochemical performances, such as constant current charge/discharge curvesand AC electrochemical impedance spectroscopy, were carried out using electrochemical workstation (Shanghai Chenhua Instrument Co., Ltd., CHI660e).

3. Results and discussion

Garnet-type $Li_{6.75}La_3Al_{0.25}Zr_2O_{12}$ (LLAZO) has been synthesized by the solid phase sintering, since trivalent Al-ion can reduce sintering temperature, stabilize cubic garnet phase and increase Li-ion conductivity.[37,38] The powder X-ray diffraction (XRD) pattern of the LLAZO pellet shown in Fig. 1 and Fig. S1 matches that of cubic garnet-phase $Li_5La_3Nb_2O_{12}$ (PDF #80-0457), and the cross-section scanning electronic microscopy (SEM, Fig. S2) displays uniform primary grains with the size of 0.5 – 10 μm. The mixed powder of garnet and lithium cobaltate with a mass ratio of 1:1 was annealed at 873 K for 6 hours, and corresponding XRD pattern is shown in Fig. 1A. A large number of new diffraction peaks are observed at 18.5°, 28.6°, 33.0°, 47.6° and 56.4°, because of the spontaneous chemical reaction between $LiCoO_2$ and garnet electrolyte material. Therefore, black lithium cobaltate ($LiCoO_2$) powder was used to modify the surface of fresh garnet ceramics at 873 K for 6 hours, and the modified Co@SSE@Co electrolyte displays several characteristic diffraction peaks of the cobalt-oxygen compounds ($Li_{1-x}Co_{1-y}O_2$) in Fig. 1B. Even if the garnet electrolyte and $LiCoO_2$ were kept in contact at room temperature for 48 hours, the impurity peaks were still clearly observed in Fig. S3. In Fig. 1C, the Co@SSE@Co electrolyte modified by cobalt-oxygen compounds changes from milky white to light yellow. As shown in the cross-section scanning electronic microscopy (SEM) image in Fig. 1D, nano-scale

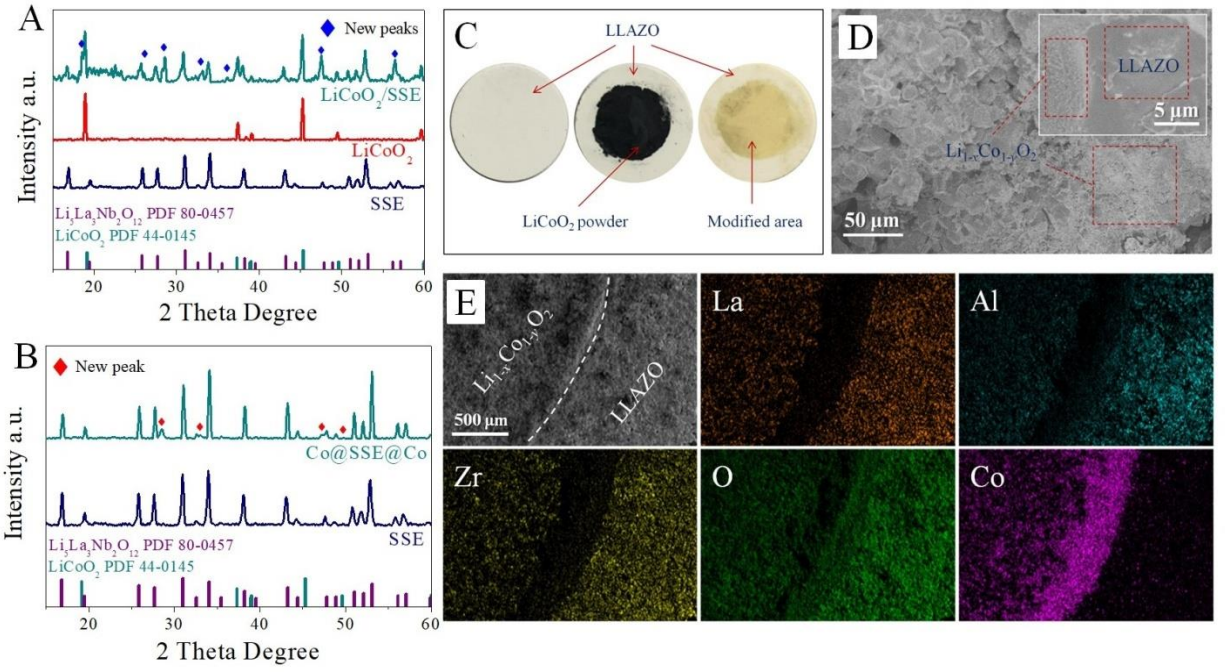

Fig. 1 Characterization of the garnet LLAZO solid-state electrolyte. (A) XRD pattern of a mixed powder with an $m_{garnet}/m_{lithiumcobaltate}$ mass ratio of 1:1 calcined at 873 K for 6 hours. (B) XRD pattern of the Co@SSE@Co garnet ceramic calcined at 873 K for 6 hours. (C) Digital photos of garnet electrolytes. (D) SEM image for cross section of the Co@SSE@Co pellet. (E) EDS mapping of the Co@SSE@Co surface.

$Li_{1-x}Co_{1-y}O_2$ primary particles diffuse inward along the garnet grain boundary at 873 K, and finally homogeneously distribute the inner interface of the solid-state electrolyte. Fig. 1E exhibits the energy dispersive spectroscopy (EDS) elemental mapping of the surface of the Co@SSE@Co electrolyte. The Co elemental mapping further confirms the continuous modification area of the cobalt-oxygen compounds.

X-ray photoelectron spectroscopy (XPS) analysis was performed to further confirm the chemical modification of the garnet surface by lithium cobaltate. The Co@SSE@Co electrolyte exhibits two sets of signal peaks at 794 – 779 and 532 eV corresponding to Co 2p and O 1s core levels in Fig. 2A, respectively. O 1s core spectrum of the Co@SSE@Co electrolyte can be cure-fitted to two peaks at 531.7 and 529.6 eV that belong to the garnet electrolyte and $Li_{1-x}Co_{1-y}O_2$ materials, respectively. Compared with pure $LiCoO_2$ powder, the signal peaks of Co2p are reduced from three to two for the Co@SSE@Coelectrolyte, and the deviation of the high bond energy direction is 0.8 – 0.9 eV. Li-ion conductivity of the garnet solid-state electrolyte is evaluated by electrochemical impedance spectroscopy (EIS) with gold electrodes at temperatures of 310 – 333 K. As shown in Fig. 2B, all the Nyquist plots are composed of two semicircles at high-medium frequency and a tilted low-frequency tail. The intersection of the second arc and the *x*-axis at high frequencies can be assigned to the bulk resistance of LLAZO, whereas the depressed arc is associated with the grain boundary response. Total Li-ion conductivity of the as-prepared $Li_{6.75}La_3Al_{0.25}Zr_2O_{12}$ electrolyte (Fig. S4) is equal to 0.14 mS cm^{-1} at 310 K, while the symmetrical Au/Co@SSE@Co/Au device shows a larger value of 0.21 mS cm^{-1}.[39,40] The activation energy of the Co@SSE@Co electrolyte decreased from 0.47 eV to 0.35 eV in Fig. 2C.

The $Li/LiCoO_2$/SSE devices were assembled in an argon atmosphere as shown in Fig. 3A, and then placed under a pressure of 1 MPa at room temperature for 48 hours. It is difficult to observe black lithium cobaltate on the garnet and Li metal. In contrast, a large amount of residual $LiCoO_2$ powder is clearly observed in the stainless steel/$LiCoO_2$/SSE device (Fig. S5). Therefore, Li metal is beneficial to the physical modification of the garnet electrolyte, which is further confirmed by the weakened diffraction peaks of lithium cobaltate (Fig. 3B).

The fresh garnet SSE, Co@SSE@Co and Li/Co@SSE@Co/Li samples were carried out by using XRD in Fig. 4A. The featured XRD peaks of the cubic LLAZO and Li metal are maintained for the Li/Co@SSE@Co/Li sample. However, the diffraction peak derived from the cobalt-oxygen compounds at 28.6, 33.0, 47.5 and 49.7° disappeared completely for the Li/Co@SSE@Co/Li. This further shows that Li metal can promote the chemical reaction cobalt-oxygen compounds and the garnet electrolyte, and finally achieve Co doping of the surface of the garnet electrolyte. The interface morphology was carried out by SEM, as shown in Figs. 4B-D, which compares the Li wetting behavior of garnet SSE with/without a $Li_{1-x}Co_{1-y}O_2$ coating. A large gap exists in the Li/garnet interface even after Li metal is pressed onto the LLAZO SSE at 453 K. Li metal electrode is contacted with the garnet Co@SSE@Co electrolyte at room temperature for 48 hours. From the SEM images in Figs. 4C and D, we can clearly

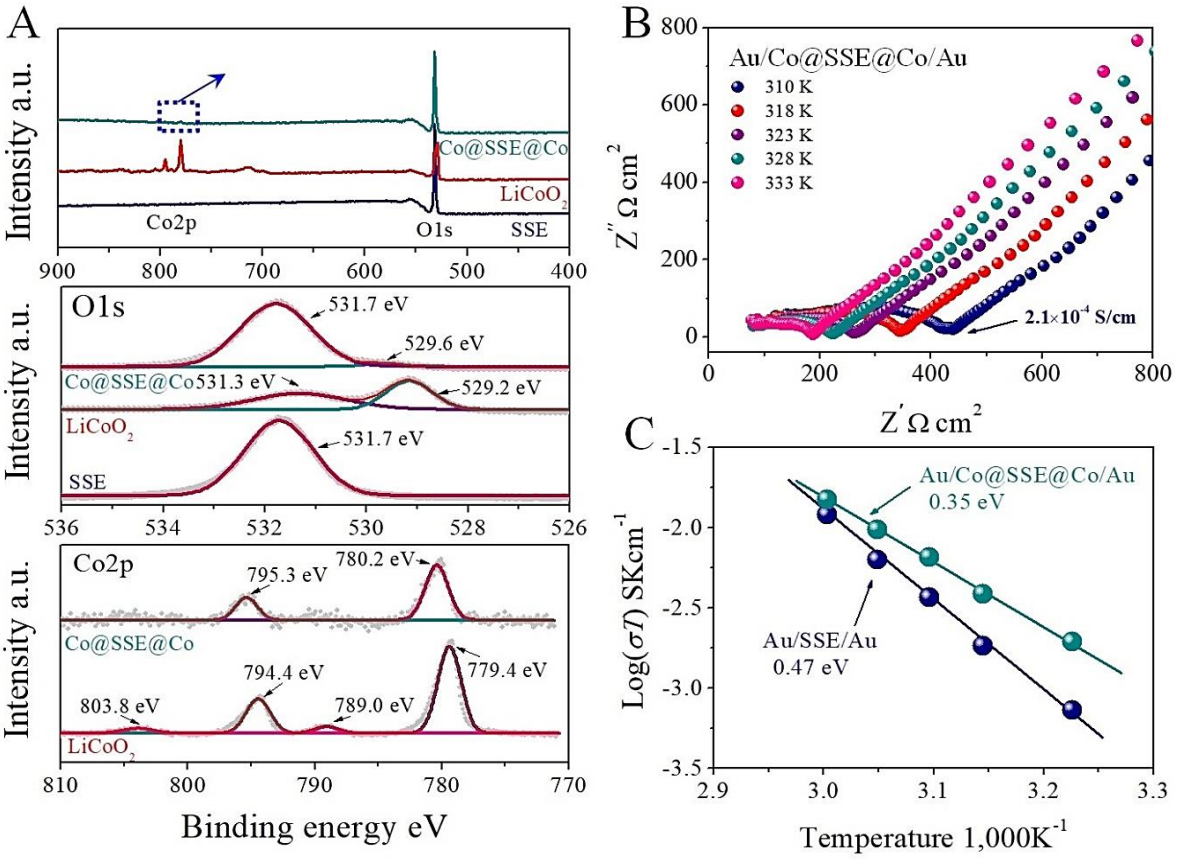

Fig. 2 XPS (A), EIS (B)and Arrhenius plot (C) of the as-prepared Co@SSE@Co electrolyte.

see that almost all the pores on the surface of the Co@SSE@Co garnet have been filled with Li metal, indicating that the $Li_{1-x}Co_{1-y}O_2$ coating layer can significantly improve the wettability of the garnet electrolyte for Li metal. Inset is photo of melted Li metal on top of the garnet surface (Fig. 4D), demonstrating classical wetting behavior for the modified garnet.

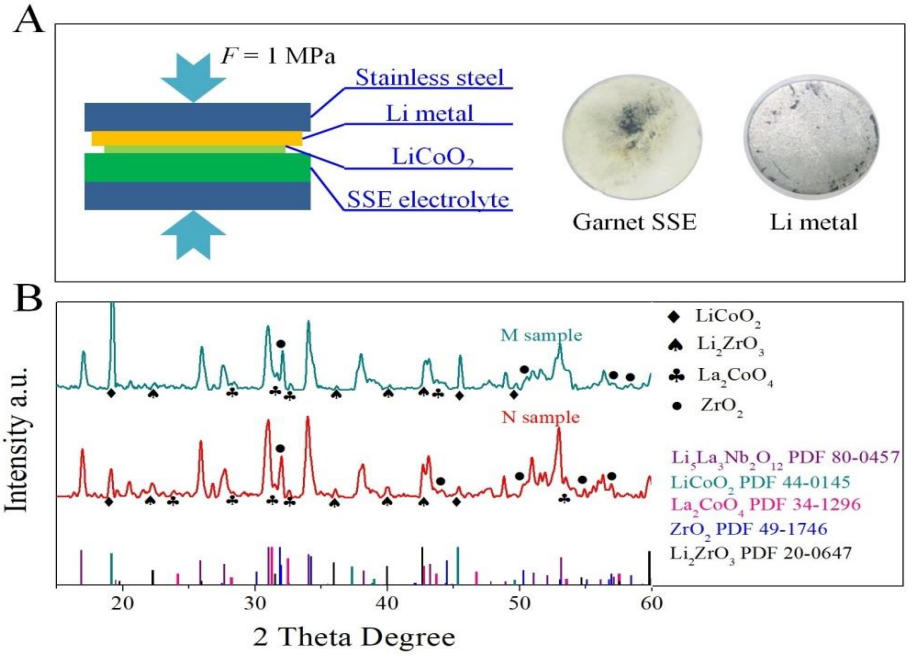

Fig. 3 Digital photos (A) and XRD patterns (B) of the garnet electrolytes. Note: M sample is the garnet electrolyte of the Li/$LiCoO_2$/SSE device after being placed at room temperature for 48 hours. N sample is derived from the stainless steel/$LiCoO_2$/SSE device.

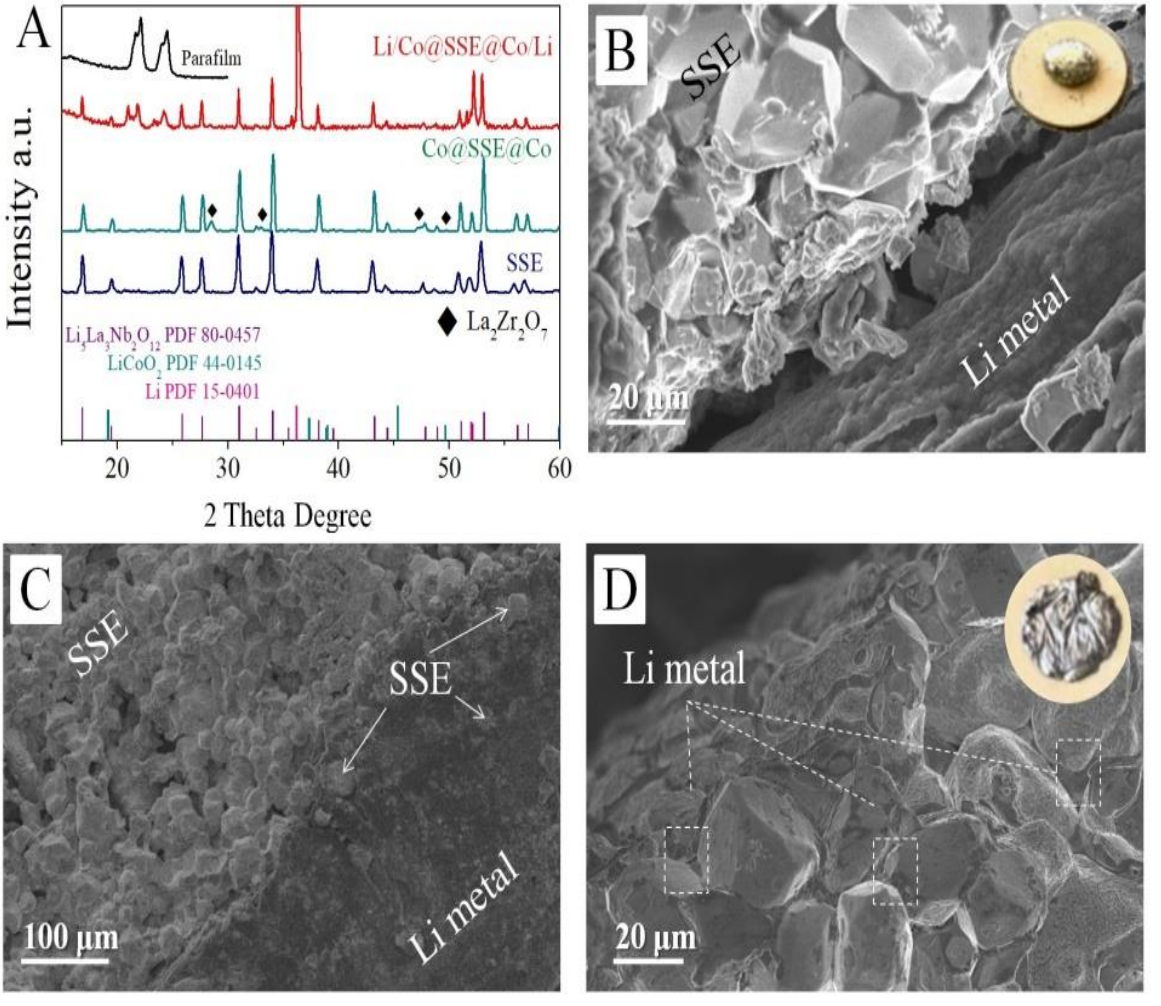

Fig. 4 Characterizations of garnet solid-state electrolyte/Li metal interface. (A) XRD patterns. (B) Cross-section SEM image of the Li/pure garnet. (C) SEM image of the Li/Co@SSE@Co/Li sample. The Co@SSE@Co electrolyte was calcined at 873 K for 6 hours. (D) SEM image of the garnet electrolyte after stripping Li metal from Li/Co@SSE@Co/Li device.

The interfacial resistance was evaluated by galvanostatically charging and discharging at a series of the constant current densities. The symmetric Li/SSE/Li battery (surface area of ~0.2 cm^2) is difficult to withstand the long-term test of 20 μA in Fig. 5A, and corresponding total resistance increases rapidly from 12,200 Ω cm^2 to 17,000 Ω cm^2. Note that the total resistance corresponds to a garnet solid-state electrolyte with a thickness of about 500 μm and

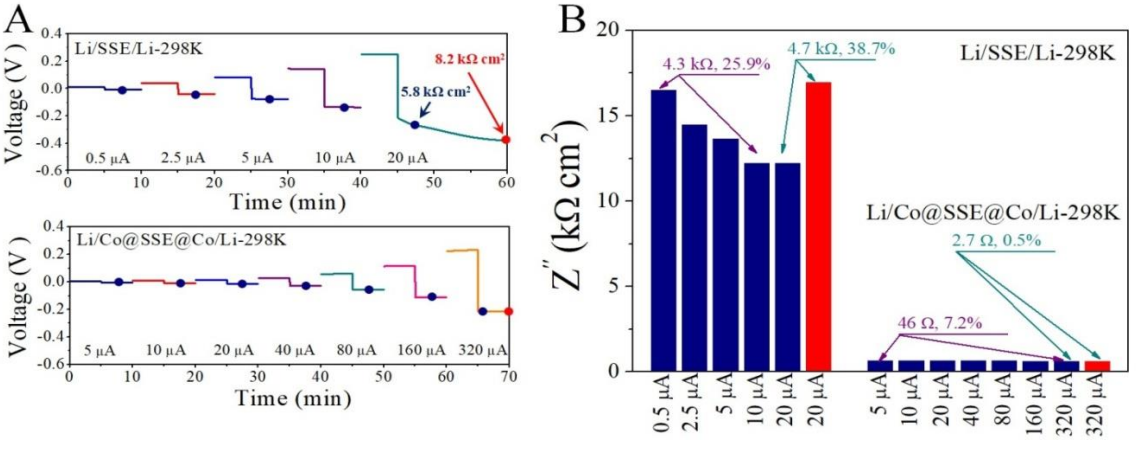

Fig. 5 Charge-discharge curves (A) and total resistances (B) of the symmetric Li/SSE/Li and Li/Co@SSE@Co/Li batteries at different current. Note: The data represent the difference and rate of change of the total resistance (Fig. 5B).

two symmetric interfaces between the garnet electrolyte and Li metal. The resistances of the LLAZO electrolyte before and after modification of the $LiCoO_2$ powder are 450 and 300 Ωrespectively, which can be calculated according to the results of Li-ion conductivity in Fig. 1. Therefore, the interface resistance of the Li/SSE/Li battery fluctuates between 5,800 Ω cm^2 and 8,200 Ω cm^2. The Li/Co@SSE@Co/Li battery is placed under a pressure of about 1 MPa at room temperature for 48 hours. The characteristic interface resistance is constant at 162 ± 12 Ω cm^2 at current densities of 5 μA to 320 μA (Fig. 5B), accounting for only 3.7% of the resistance of the Li/SSE/Li battery. The constant current charge-discharge curves fully confirm the good physical contact between Li metal and garnet electrolyte.

The interfacial resistances were evaluated by electrochemical impedance spectroscopy (EIS) and voltage profile depicting the Li plating/striping behavior for Li/garnet SSE/Li symmetric batteries. Fig. 6A is a schematic diagram of the basic structure of the symmetric batteries. The newly-made Li/garnet SSE/Li batteries are placed under a pressure of 1 MPa at 298 K for 48 hours to reduce the influence of the assembly process on the contact of the Li/SSE interface. The total resistance of the Li/SSE/Li decreases from 34,000 Ω cm^2(under 1MPa for 1 hour) to 20,000 Ω cm^2(under 1MPa for 48 hours) in Fig. 6B; however, the resistance of the symmetric Li/Co@SSE@Co/Li battery is between 705 – 630 Ω cm^2. The 97% drop value of the total resistance proves that the surface/interface of the garnet chemically modified with lithium cobaltate can strengthen the infiltration ability of Li metal. The heat treatment temperature of the symmetric batteries is increased from 298 K to 413 K. Interfacial resistances of the Li/SSE/Li battery drop from 4,800 Ω cm^2 to 2,100 Ω cm^2 in Fig. 6B, as molten Li is squeezed into the coarse pores of the garnet. For the Li/Co@SSE@Co/Li battery, it is almost impossible to reduce the interfacial resistance of 165 – 150 Ω cm^2 by hot pressing at the temperature of 298 – 413 K. In agreement with the EIS test results, Li/Co@SSE@Co/Li battery exhibits a long-term stable electrochemical striping/plating process at a 50 μA cm^{-2} current density in Fig. 6C, whereas the signal voltage of the

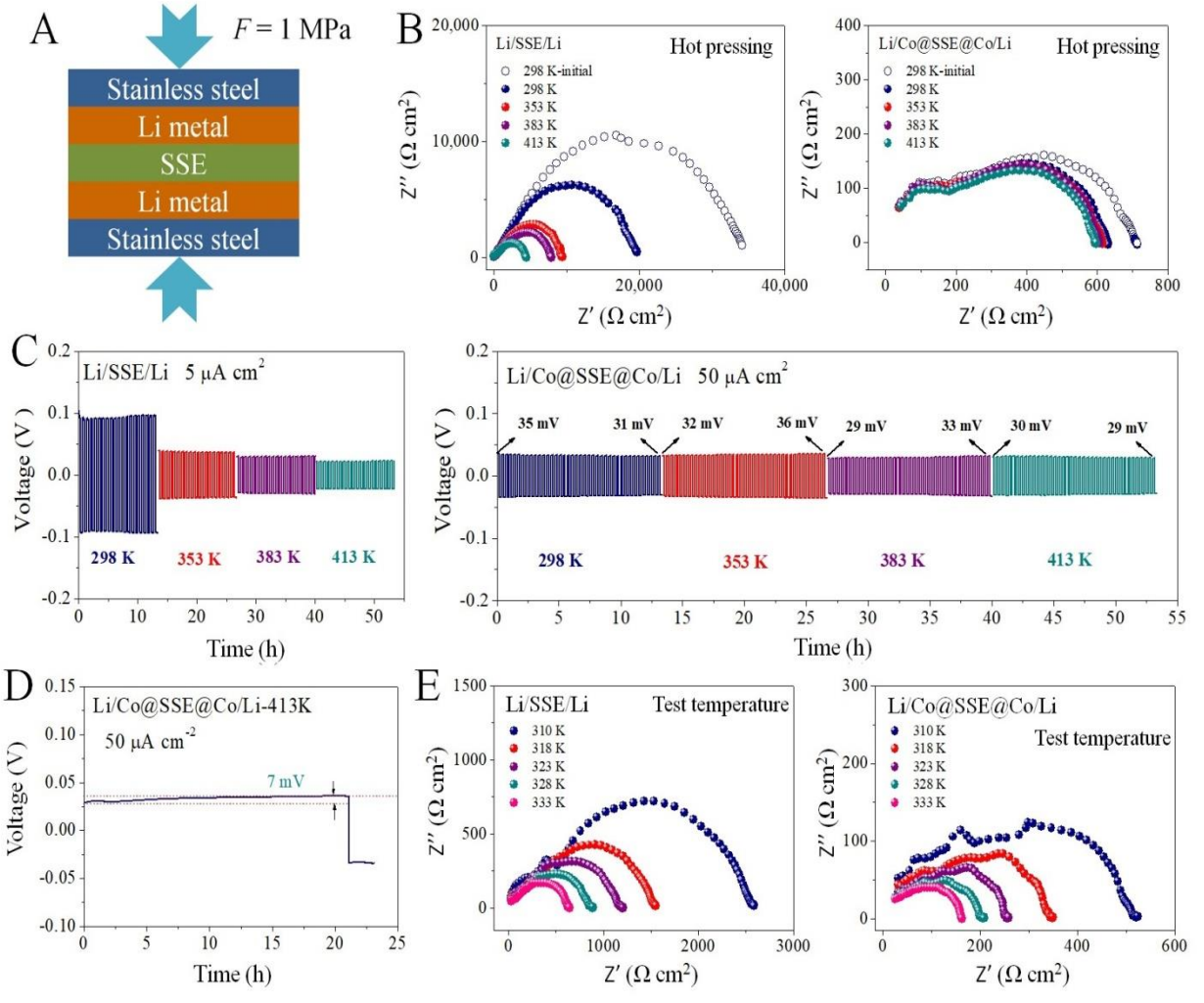

Fig. 6 Electrochemical performances of the Li/garnet SSE/Li symmetric batteries. (A) Schematic diagram of the symmetric batteries. (B) EIS spectra of the batteries after hot pressing at different temperatures. (C) Galvanostatic cycling of the symmetric batteries. (D) Li plating of the Li/Co@SSE@Co/Li battery at room temperature with a current density of 0.05 mA cm^{-2} for 20 hours. (E) Nyquist plots of the symmetric batteries at various elevated temperatures.

Li/SSE/Li battery is obviously related to the pretreatment temperature. EIS and Li plating/striping results fully show that the garnet Co@SSE@Co electrolyte has high wettability to Li metal. The symmetric Li/Co@SSE@Co/Li battery is tested at room temperature at a current density of 50 μA cm^{-2} for about 20 hours, and the D-value between the initial and cut-off voltage does not exceed 7 mV in Fig. 6D. The Li/Co@SSE@Co/Li battery presents a specific capacity of 1.0 mAh, which is equivalent to transferring 0.26 mg of Li metal to the counter electrode.

The temperature-dependent resistance was characterized using EIS for the Li/SSE/Li and Li/Co@SSE@Co/Li batteries at temperatures from 310 K to 333 K. The total resistance of the symmetric batteries decreases as the temperature increases. The intersection of the semicircle and real axis at medium-low frequency decreases in an orderly manner, indicating that the interface resistance negatively correlates with temperature. For the fully balanced Li/SSE/Li battery treated at 453 K for 12 hours, the total resistance still exceeds 600 Ω at 333 K. The total resistances of the Li/Co@SSE@Co/Li are equal to 510, 350, 275, 204 and 170 Ω at the temperature of 310, 318, 323, 328, 333 K, respectively.

4. Conclusions

In summary, we have reported a novel strategy to solve the interface contact issue between Li metal electrode and garnet solid-state electrolyte toward all-solid-state Li metal batteries. Cobalt oxide nanoparticles diffuse inward along the grain boundary of the garnet electrolyte until these primary particles are evenly distributed on the inner interface of the garnet. Li metal perfectly penetrates into the pores of the garnet electrolyte with the help of cobalt-oxygen compounds, so that the point contact between the Li metal and the garnet electrolyte (Fig. 4B) is transformed into a three-dimensional contact (Fig. 4D). The total resistance, which contributes to a garnet solid-state electrolyte and two symmetric contact interfaces, drops from 20,000 Ω $cm^2$of the Li/SSE/Li symmetric battery to 630 Ω $cm^2$of the Li/Co@SSE@Co/Li. The Li/Co@SSE@Co/Li battery exhibits a series of stable signal voltage platforms at current densities of 0.025 – 1.6 mA cm^{-2}. The maximum voltage fluctuation is less than 7 mV for the modified battery during 160 Li-striping/plating cycles at 0.25 mA cm^{-2}. Our surface treatment technique no longer relies on hot pressing under an inert atmosphere or expensive manufacturing technology to produce metastable nano-coating on the surface of garnet. It will inspire more effective strategies to overcome the interface problem of the garnet electrolyte and facilitate the application of the all-solid-state Li metal batteries.

Acknowledgements

This work was supported by the Finance Science and Technology Project of Hainan Province (No. ZDYF2021SHFZ102 and ZDYF2020205), National Youth Talent Support Program, Hainan Science and Technology Major Project (No. ZDKJ2019013), National Natural Science Foundation of China (No. 51775152, 61761016, 22065012 and U1967213), National Key R&D Program of China (No. 2018YFE0103500), Start-up Research Foundation of Hainan University (No. KYQD(ZR)1911), and Project Supported by Open Project of State Key Laboratory of Marine Resource Utilization in South China Sea (Hainan University) (No. MRUKF2021025).

Conflict of Interest

The authors declare no conflict of interest.

Supporting information

Applicable

Reference

[1] H. Duan, Y.-X. Yin, Y. Shi, P.-F. Wang, X.-D. Zhang, C.-P. Yang, J.-L. Shi, R. Wen, Y.-G. Guo, L.-J. Wan, Dendrite-free Li-metal battery enabled by a thin asymmetric solid electrolyte with engineered layers, *Journal of the American Chemical Society*, 2018, **140**, 82-85, doi: 10.1021/jacs.7b10864.

[2] X.-C. Zhao, P. Yang, L.-J. Yang, Y. Cheng, H.-Y. Chen, H. Liu, G. Wang, V. Murugadoss, S. Angaiah, Z. Guo, Enhanced electrochemical performance of Cu^{2+} doped TiO_2 nanoparticles for lithium-ion battery, *ES Materials & Manufacturing*, 2018, **1**, 67-71doi: 10.30919/esmm5f109.

[3] A. Perea, M. Dontigny, K. Zaghib, Safety of solid-state Li metal battery: solid polymer versus liquid electrolyte, *Journal of Power Sources*, 2017, **359**, 182-185, doi: 10.1016/j.jpowsour.2017.05.061.

[4] A. M. Hafez, J. Sheng, D. Cao, Y. Chen, H. Zhu, Flexible lithium metal anode featuring ultrahigh current density stability with uniform deposition and dissolution, *ES Energy & Environment*, 2019, **5**, 85-93 doi: 10.30919/esee8c311.

[5] S. G. Sayyed, A. V. Shaikh, D. P. Dubal, H. M. Pathan, Paving the way towards Mn_3O_4 based energy storage systems, *ES Energy & Environment*, 2021, **14**, 3-21, doi: 10.30919/esee8c522.

[6] J.-R. Wang, M.-M. Wang, X.-D. He, S. Wang, J.-M. Dong, F. Chen, A. Yasmin, C.-H. Chen, A lithiophilic 3D conductive skeleton for high performance Li metal battery, *ACS Applied Energy Materials*, 2020, **3**, 7265-7271, doi: 10.1021/acsaem.0c00055.

[7] G. Li, Z. Liu, Q. Huang, Y. Gao, M. Regula, D. Wang, L.-Q. Chen, D. Wang, Stable metal battery anodes enabled by polyethylenimine sponge hosts by way of electrokinetic effects, *Nature Energy*, 2018, **3**, 1076-1083, doi: 10.1038/s41560-018-0276-z.

[8] A. Deshpande, L. Kariyawasam, P. Dutta, S. Banerjee, Enhancement of lithium-ion mobility in ionic liquid electrolytes in presence of additives, *The Journal of Physical Chemistry C*, 2013, **117**, 25343-25351, doi: 10.1021/jp409498w.

[9] J. Xia, S. L. Glazier, R. Petibon, J. R. Dahn, Improving linear alkyl carbonate electrolytes with electrolyte additives, *Journal of the Electrochemical Society*, 2017, **164**, A1239-A1250, doi: 10.1149/2.1321706jes.

[10] W.-T. Whang, C.-L. Lu, Effects of polymer matrix and salt concentration on the ionic conductivity of plasticized polymer electrolytes, *Journal of Applied Polymer Science*, 1995, **56**, 1635-1643, doi: 10.1002/app.1995.070561214.
[11] J. Naik, R. F. Bhajantri, V. Hebbar, S. G. Rathod, Influence of ZrO_2 filler on physico-chemical properties of PVA/$NaClO_4$ polymer composite electrolytes, *Advanced Composites and Hybrid Materials*, 2018, **1**, 518-529, doi: 10.1007/s42114-018-0030-9.
[12] G.-H. Dong, F.-L. Guo, Z. Sun, Y.-Q. Li, S.-F. Song, C.-H. Xu, P. Huang, C. Yan, N. Hu, S.-Y. Fu, Short carbon fiber reinforced epoxy-ionic liquid electrolyte enabled structural battery via vacuum bagging process, *Advanced Composites and Hybrid Materials*, 2022, **5**, 1799-1811, doi: 10.1007/s42114-022-00436-z.
[13] A. Hayashi, H. Muramatsu, T. Ohtomo, S. Hama, M. Tatsumisago, Improvement of chemical stability of Li_3PS_4 glass electrolytes by adding M_xO_y (M = Fe, Zn, and Bi) nanoparticles, *Journal of Materials Chemistry A*, 2013, **1**, 6320, doi: 10.1039/c3ta10247e.
[14] J.-M. Hu, B. Wang, Y. Ji, T. Yang, X. Cheng, Y. Wang, L.-Q. Chen, Phase-field based multiscale modeling of heterogeneous solid electrolytes: applications to nanoporous Li_3PS_4, *ACS Applied Materials & Interfaces*, 2017, **9**, 33341-33350, doi: 10.1021/acsami.7b11292.
[15] M. Matsuo, S.-I. Orimo, Lithium fast-ionic conduction in complex hydrides: review and prospects, *Advanced Energy Materials*, 2011, **1**, 161-172, doi: 10.1002/aenm.201000012.
[16] W. Li, J. Liang, M. Li, K. R. Adair, X. Li, Y. Hu, Q. Xiao, R. Feng, R. Li, L. Zhang, S. Lu, H. Huang, S. Zhao, T.-K. Sham, X. Sun, Unraveling the origin of moisture stability of halide solid-state electrolytes by in situ and Operando synchrotron X-ray analytical techniques, *Chemistry of Materials*, 2020, **32**, 7019-7027, doi: 10.1021/acs.chemmater.0c02419.
[17] Y. Li, W. Zhou, S. Xin, S. Li, J. Zhu, X. Lü, Z. Cui, Q. Jia, J. Zhou, Y. Zhao, J. B. Goodenough, Fluorine-doped antiperovskite electrolyte for all-solid-state lithium-ion batteries, *Angewandte Chemie*, 2016, **128**, 10119-10122, doi: 10.1002/ange.201604554.
[18] J. Kang, H. Chung, C. Doh, B. Kang, B. Han, Integrated study of first principles calculations and experimental measurements for Li-ionic conductivity in Al-doped solid-state $LiGe_2(PO_4)_3$ electrolyte, *Journal of Power Sources*, 2015, **293**, 11-16, doi: 10.1016/j.jpowsour.2015.05.060.
[19] B. E. Francisco, C. R. Stoldt, J.-C. M'Peko, Lithium-ion trapping from local structural distortions in sodium super ionic conductor (NASICON) electrolytes, *Chemistry of Materials*, 2014, **26**, 4741-4749, doi: 10.1021/cm5013872.
[20] Z. Liu, X. Tian, M. Liu, S. Duan, Y. Ren, H. Ma, K. Tang, J. Shi, S. Hou, H. Jin, G. Cao, Direct ink writing of $Li_{1.3}Al_{0.3}Ti_{1.7}(PO_4)_3$-based solid-state electrolytes with customized shapes and remarkable electrochemical behaviors, *Small*, 2021, **17**, 2002866, doi: 10.1002/smll.202002866.
[21] D.-L. Xiao, J. Tong, Y. Feng, G.-H. Zhong, W.-J. Li, C.-L. Yang, Improved performance of all-solid-state lithium batteries using LiPON electrolyte prepared with Li-rich sputtering target, Solid State Ionics, 2018, **324**, 202-206, doi: 10.1016/j.ssi.2018.07.011.
[22] T. Famprikis, J. Galipaud, O. Clemens, B. Pecquenard, F. Le Cras, Composition dependence of ionic conductivity in LiSiPO(N) thin-film electrolytes for solid-state batteries, *ACS Applied Energy Materials*, 2019, **2**, 4782-4791, doi: 10.1021/acsaem.9b00415.
[23] A. Sharafi, E. Kazyak, A. L. Davis, S. Yu, T. Thompson, D. J. Siegel, N. P. Dasgupta, J. Sakamoto, Surface chemistry mechanism of ultra-low interfacial resistance in the solid-state electrolyte $Li_7La_3Zr_2O_{12}$, *Chemistry of Materials*, 2017, **29**, 7961-7968, doi: 10.1021/acs.chemmater.7b03002.
[24] X. Wu, J. Zhong, H. Zhang, H. Liu, J. Mai, S. Shi, Q. Deng, N. Wang, Garnet $Li_7La_3Zr_2O_{12}$ solid-state electrolyte: environmental corrosion, countermeasures and applications, *ES Energy & Environment*, 2021, **14**, 22-33, doi: 10.30919/esee8c494.
[25] F. Han, Y. Zhu, X. He, Y. Mo, C. Wang, Electrochemical stability of $Li_{10}GeP_2S_{12}$ and Li_7La_3 Zr_2O_{12} solid electrolytes, *Advanced Energy Materials*, 2016, **6**, 1501590, doi: 10.1002/aenm.201501590.
[26] D. Rettenwander, G. Redhammer, F. Preishuber-Pflügl, L. Cheng, L. Miara, R. Wagner, A. Welzl, E. Suard, M. M. Doeff, M. Wilkening, J. Fleig, G. Amthauer, Structural and electrochemical consequences of Al and Ga cosubstitution in $Li_7La_3Zr_2O_{12}$ solid electrolytes, *Chemistry of Materials*, 2016, **28**, 2384-2392, doi: 10.1021/acs.chemmater.6b00579.
[27] X. Tao, Y. Liu, W. Liu, G. Zhou, J. Zhao, D. Lin, C. Zu, O. Sheng, W. Zhang, H.-W. Lee, Y. Cui, Solid-state lithium-sulfur batteries operated at 37 °C with composites of nanostructured $Li_7La_3Zr_2O_{12}$/carbon foam and polymer, *Nano Letters*, 2017, **17**, 2967-2972, doi: 10.1021/acs.nanolett.7b00221.
[28] Y. Jin, P. J. McGinn, Bulk solid state rechargeable lithium ion battery fabrication with Al-doped $Li_7La_3Zr_2O_{12}$ electrolyte and $Cu_{0.1}V_2O_5$ cathode, *Electrochimica Acta*, 2013, **89**, 407-412, doi: 10.1016/j.electacta.2012.11.059.
[29] K. K. Fu, Y. Gong, B. Liu, Y. Zhu, S. Xu, Y. Yao, W. Luo, C. Wang, S. D. Lacey, J. Dai, Y. Chen, Y. Mo, E. Wachsman, L. Hu, Toward garnet electrolyte-based Li metal batteries: an ultrathin, highly effective, artificial solid-state electrolyte/metallic Li interface, *Science Advances*, 2017, **3**, e1601659, doi: 10.1126/sciadv.1601659.
[30] W. Luo, Y. Gong, Y. Zhu, Y. Li, Y. Yao, Y. Zhang, K. K. Fu, G. Pastel, C.-F. Lin, Y. Mo, E. D. Wachsman, L. Hu, Reducing interfacial resistance between garnet-structured solid-state electrolyte and Li-metal anode by a germanium layer, *Advanced Materials*, 2017, **29**, 1606042, doi: 10.1002/adma.201606042.
[31] X. Han, Y. Gong, K. Fu, X. He, G. T. Hitz, J. Dai, A. Pearse, B. Liu, H. Wang, G. Rubloff, Y. Mo, V. Thangadurai, E. D. Wachsman, L. Hu, Negating interfacial impedance in garnet-based solid-state Li metal batteries, *Nature Materials*, 2017, **16**, 572-579, doi: 10.1038/nmat4821.
[32] C. Wang, Y. Gong, B. Liu, K. Fu, Y. Yao, E. Hitz, Y. Li, J. Dai, S. Xu, W. Luo, E. D. Wachsman, L. Hu, Conformal, nanoscale ZnO surface modification of garnet-based solid-state

electrolyte for lithium metal anodes, *Nano Letters*, 2017, **17**, 565-571, doi: 10.1021/acs.nanolett.6b04695.
[33] X. Ma, Y. Xu, B. Zhang, X. Xue, C. Wang, S. He, J. Lin, L. Yang, Garnet Si-$Li_7La_3Zr_2O_{12}$ electrolyte with a durable, low resistance interface layer for all-solid-state lithium metal batteries, *Journal of Power Sources*, 2020, **453**, 227881, doi: 10.1016/j.jpowsour.2020.227881.
[34] C. Yang, H. Xie, W. Ping, K. Fu, B. Liu, J. Rao, J. Dai, C. Wang, G. Pastel, L. Hu, An electron/ion dual-conductive alloy framework for high-rate and high-capacity solid-state lithium-metal batteries, *Advanced Materials*, 2019, **31**, 1804815, doi: 10.1002/adma.201804815.
[35] J. Duan, W. Wu, A. M. Nolan, T. Wang, J. Wen, C. Hu, Y. Mo, W. Luo, Y. Huang, Solid-state batteries: lithium-graphite paste: an interface compatible anode for solid-state batteries, *Advanced Materials*, 2019, **31**, 1970068, doi: 10.1002/adma.201970068.
[36] Y. Gao, D. Wang, Y. C. Li, Z. Yu, T. E. Mallouk, D. Wang, Salt-based organic-inorganic nanocomposites: towards A stable lithium metal/$Li_{10}GeP_2S_{12}$ solid electrolyte interface, *Angewandte Chemie International Edition*, 2018, **57**, 13608-13612, doi: 10.1002/anie.201807304.
[37] X. Zhao, H. Zhang, Y. Yuan, Y. Ren, N. Wang, Ultra-fast and stable extraction of Li metal from seawater, *Chemical Communications*, 2020, **56**, 1577-1580, doi: 10.1039/c9cc08927f.
[38] H. Zhang, Y. Ren, X. Wu, N. Wang, An interface-modified solid-state electrochemical device for lithium extraction from seawater, *Journal of Power Sources*, 2021, **482**, 228938, doi: 10.1016/j.jpowsour.2020.228938.
[39] K. Park, B.-C. Yu, J.-W. Jung, Y. Li, W. Zhou, H. Gao, S. Son, J. B. Goodenough, Electrochemical nature of the cathode interface for a solid-state lithium-ion battery: interface between $LiCoO_2$ and garnet-$Li_7La_3Zr_2O_{12}$, *Chemistry of Materials*, 2016, **28**, 8051-8059, doi: 10.1021/acs.chemmater.6b03870.
[40] J. Sastre, X. Chen, A. Aribia, A. N. Tiwari, Y. E. Romanyuk, Fast charge transfer across the $Li_7La_3Zr_2O_{12}$ solid electrolyte/$LiCoO_2$ cathode interface enabled by an interphase-engineered all-thin-film architecture, *ACS Applied Materials & Interfaces*, 2020, **12**, 36196–36207, doi: 10.1021/acsami.0c09777.

Author Information

Haiquan Zhang received his Ph.D. degree in Materials science from Southwest Jiaotong University. Now he works as a lecturer in the State Key Laboratory of Marine Resource Utilization in South China Sea, Hainan University. His research interests focus on lithium extraction from seawater, surface modification, chemical resistance, and Li-ion batteries.

Houji Liu, currently a Master student in the State Key Laboratory of Marine Resource Utilization in South China Sea, Hainan University. He obtained his Bachelor degree from China Three Gorges University in 2018. His research focuses on the preparation and modification of anode materials for lithium-ion batteries.

***Junping Mai**, currently a Master student in the State Key Laboratory of Marine Resource Utilization in South China Sea, Hainan University. She obtained her Bachelor degree from China Three Gorges University in 2019. Her research focuses on the new electrode materials and their application in lithium extraction from seawater.*

***Yuxi Ren**, currently a Master student in the State Key Laboratory of Marine Resource Utilization in South China Sea, Hainan University. She obtained her Bachelor degree from Nantong University in 2018. Her research focuses on the preparation and surface modification of garnet solid electrolyte.*

***Renjuan Wang** received her B.S. degree from Xiangtan University. Now she studies as a master student in the State Key Laboratory of Marine Resource Utilization in South China Sea, Hainan University since September 2020. Her research focuses on the preparation and surface modification of garnet solid electrolyte.*

***Xin Li** received his B.S. degree from Jilin Jianzhu University in 2020. Now he studies as a master student in the State Key Laboratory of Marine Resource Utilization in South China Sea, Hainan University since September 2020. His research focuses on the preparation and modification of anode materials for lithium-ion batteries.*

***Qijiu Deng** received his Ph.D. degree from the University of Electronic Science and Technology of China in 2017. He is currently a lecturer at the Xi'an University of Technology. His research interests are nanomaterials for energy conversion and storage.*

Rui-Zhi Zhang *received his Ph.D. from Shandong University in China. After completing Ph.D, he worked in Northwest University in Xi'an, China as an associate professor. In 2014, he held the position of Marie Curie Research Fellow at Queen Mary University of London. His research interests include data-driven ceramics design utilizing density functional theory and deep neural networks, and spark plasma sintering of thermoelectric ceramics and high entropy ceramics.*

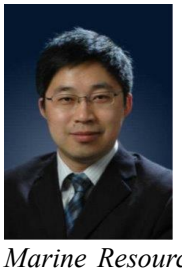

Ning Wang *obtained his Ph.D. from Tsinghua University (2007) and joined as a post-doctoral fellow at Nagoya University (2008–2010), then he worked as a visiting scholar at the University of California, Berkeley (2013–2014). He is currently a Professor of the State Key Laboratory of Marine Resource Utilization in South China Sea at Hainan University. His research interests are mainly in the field of advanced functional material preparation for uranium extraction from seawater, lithium extraction from seawater and perovskite solar cells.*